

Melt spun matrix fibers of toughened polypropylene copolymers modified by high energy electrons

Samer ALRahhal,^{1,2} Harald Brüinig,² Uwe Gohs,² Gert Heinrich^{1,2}

¹Leibniz-Institut für Polymerforschung Dresden e. V., Hohe Straße 6, Dresden 01069, Germany

²Technische Universität Dresden, Institut für Werkstoffwissenschaft, Dresden 01062, Germany

Correspondence to: S. ALRahhal (E-mail: rahhal@ipfdd.de)

ABSTRACT: Binary blends of polypropylene (PP) and ethylene-octene copolymer (EOC) are prepared by continuous electron-induced reactive processing at various mass ratios of the blend components and various doses without adding of any grafting agents. The influence of mass ratio and dose is investigated in order to get the optimum processing behavior of toughened PP as well as optimum properties of resulting fibers. It is found that toughened PP with a PP/EOC blend ratio of 97.5–2.5 mass % can be used advantageously as a matrix component for the process of online spinning of glass fiber/toughened PP hybrid yarns. Such hybrid yarns belong to one of the most advanced production methods for the manufacturing of fiber reinforced thermoplastic composites with an increased mechanical performance. © 2016 Wiley Periodicals, Inc. *J. Appl. Polym. Sci.* **2016**, *133*, 44011.

KEYWORDS: blends; composites; fibers; thermoplastics; viscosity and viscoelasticity

Received 8 March 2016; accepted 4 June 2016

DOI: 10.1002/app.44011

INTRODUCTION

Polypropylene (PP) is known as a notch-sensitive semicrystalline thermoplastic with a number of desired properties, such as low cost and low density.¹ However, its application as a matrix for endless fiber reinforced composite material is limited because of its low stiffness and high brittleness at temperatures below room temperature. To improve the impact toughness and the low temperature properties, PP is blended with various elastomers, for example, ethylene–propylene rubber, styrene–butadiene rubber, and ethylene–propylene–diene rubber.² Recently, blends of PP and ethylene-octene copolymers (EOCs) have gained enormous attention in engineering applications, such as automotive, airplanes, and wind turbine industry.^{1,5} EOCs are metallocene-based elastomers with unique molecular characteristics. Their physical properties span the range between thermoplastics and elastomers. They have a narrow molecular mass distribution and a controlled comonomer distribution. Furthermore, they combine a high tensile strength with rubbery properties.³

The polymer modification with high energy electrons is often used in industrial applications for functionalization, degradation, crosslinking, grafting, and curing of polymeric materials.⁴ This method belongs to the group of chemical modification of polymers. It uses the spatial and temporal precise input of electron energy to modify polymers and their compounds.^{5,6} In addition, no chemical initiators are used, and therefore, unde-

sired side reactions can be minimized. Moreover, the application restrictions of thermoplastics in sensitive areas, such as medical devices and food packaging, could be eliminated. Krause *et al.*^{7,8,17} demonstrated that an electron beam (EB) treatment of PP without adding of cross-linking agents has two effects on the molecular structure of the single polymers, namely the reduction of their molar mass (chain scission) and the formation of chain branches, which are located mainly in the amorphous regions of the polymer material. The ratio of chain scission to branching depends on the applied treatment conditions as well as on material parameters of the PP used.⁸ It has been reported by Zaharah *et al.*¹⁰ and Krause *et al.*¹⁷ that isotactic PP can be branched at low absorbed doses by adding bifunctional monomers (graft copolymer). A procedure to modify the molecular structure of an initially linear PP to high melt strength PP by EB treatment was described by DeNicola¹¹ and Scheve *et al.*^{12,13} The modified PP showed a higher strain hardening and an improved storage modulus than the unmodified one. This is caused by increased entanglements between the molecular chains. Another way to improve the strain hardening behavior of PP in uniaxial elongation can be achieved by adding the styrene units as grafting chain onto PP under the presence of free radical initiators.¹⁸

Blending of PP with elastomers leads to an improved impact toughness of the blends but to reduced values of *E*-modulus and tensile strength in comparison to pure PP.^{5,16} Electron-

induced reactive processing (EIREP) enables the preparation of PP/rubber blends with an increased tensile strength and enhanced mechanical properties.^{9,16} The *in situ* melt spinning of glass fiber/PP hybrid yarns enables the combination of glass and PP filaments in one processing step without damage of glass fiber as well as with adjusted impregnation of glass and PP filaments.^{14,15} Although this developed technology has unique advantages, the limited stiffness and impact toughness of the PP matrix is still a challenge. The present work aims on the preparation of melt-spinnable PP/EOC blends for the subsequent *in situ* melt spinning of glass fiber/PP hybrid yarns process. The intention is to understand the effect of PP/EOC blend ratio and absorbed dose during EIREP on the melt spinning behavior and performance of PP/EOC blend fibers.

EXPERIMENTAL

Materials

Isotactic PP HG455FB [density 0.908 g cm⁻³ at 23 °C; MFI: 23 g/10 min (230 °C/2.16 kg); M_n : 84,800 g mol⁻¹; M_w : 223,900 g mol⁻¹; and $M_w/M_n = 2.64$] was obtained from Borealis (Düsseldorf, Germany). The EOC Engage 8100 [density 0.870 g cm⁻³ at 23 °C; comonomer (octene) content: 23 mol %; MFI: 1.0 g/10 min (190 °C/2.16 kg); M_n : 89,700 g mol⁻¹; M_w : 138,000 g mol⁻¹; $M_w/M_n = 1.54$] was procured from Dow Chemical, USA.

METHODS

EB Irradiation

A pilot plant for continuous EIREP (Figure 1) was used to prepare PP/EOC blends with different PP/EOC mass ratios at a throughput of 2.7 kg h⁻¹.²⁰ The average processing temperature was 180 °C. The rotor speed was set to 60 revolutions per minute. The authors used a nitrogen atmosphere in order to reduce the degradation of PP. The dose amounted to 3, 6, and 12 kGy. PP/EOC blends with the mass ratios of 97.5/2.5, 95/5, and 90/10 were labeled with A, B, and C, respectively. The numbers behind the capital letters describe the dose in kGy.

Characterization of Modified Blends

The authors studied the melt spinning behavior of PP/EOC blends by investigations of their rheological and thermal properties. Finally, melt spinning tests were performed using a self-constructed piston-type spinning device and an extruder melt spinning equipment.

Dynamic Rheological Measurements. Oscillating measurements on the molten blends in nitrogen atmosphere were carried out on a rotational rheometer (ARES-G2, plate-to-plate arrangement, plate diameter 25 mm, gap width 1.5 mm). The frequency sweep measurements were performed at 200 °C within an angular frequency range of (0.1–100 rad s⁻¹) at constant strain amplitude of 10%. Strain amplitude of 10% was selected to ensure the measurements in the linear viscoelastic region. All frequency sweep tests started at 100 rad s⁻¹. The temperature sweep measurements were carried out at 1 rad s⁻¹ within a temperature range of (170–260 °C) at a constant strain amplitude of 3%. Regarding the thermal stability, a time sweep measurement (1–1800 s) was carried out at 1 rad s⁻¹ and 210 °C. For all samples, the absolute value of complex viscosity was also determined in a cooling run (starting at 240 °C, cooling rate

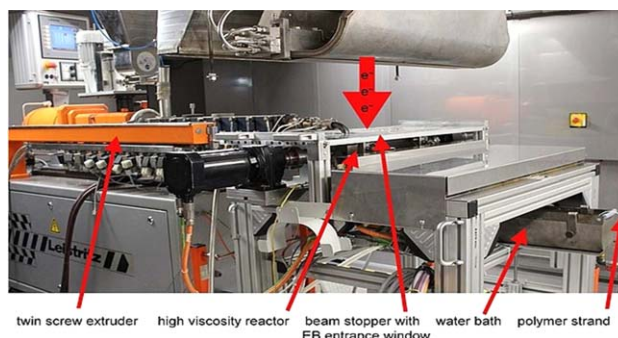


Figure 1. Pilot plant for electron induced reactive processing (EIREP) (designed by IPF, Dresden, Germany). [Color figure can be viewed in the online issue, which is available at wileyonlinelibrary.com.]

5 K min⁻¹, and frequency 10 rad s⁻¹). The absolute values of complex melt viscosities were calculated using the experimental data of the storage and loss moduli measured as a function of shear frequency and/or temperature.

Differential Scanning Calorimetry. Thermal properties were analyzed by differential scanning calorimetry (DSC) using a calorimeter DSC Q1000 (TA Instrument, Germany.) in the temperature range from -80 to 200 °C at a heating rate of 10 K min⁻¹ under nitrogen atmosphere. The data for a cycle of first heating, cooling, and second heating were measured. Glass transition (T_g), melting (T_m), and crystallization temperatures (T_c) as well as the melting and crystallization enthalpies were determined. The degree of crystallinity of PP was calculated using the following relation:

$$X = \frac{\Delta H_f}{\Delta H_{c100\%}} \times 100\% \quad (1)$$

where X is the degree of crystallinity (%), ΔH_f is the apparent melting enthalpy of crystallization, $\Delta H_{c100\%}$ is the value of the enthalpy of crystallization of 100% crystalline sample (209 J g⁻¹ for PP).¹⁶ The melting temperature (T_m) was determined from the second heating, and the crystallization temperature (T_c) was calculated from the cooling cycle.

Single Fiber Preparation by Piston Spinning

The melt spinning of single fibers were carried out with a piston melt spinning device (Figure 2) using small sample masses of 10 g. The investigations were performed at various mass throughputs (Q) 0.1, 0.2, 0.3, and 0.6 g min⁻¹, spinning temperatures (T) (180, 190, 200, and 210 °C), and take-up speeds (V) (500, 1000, 1500, and 2000 m min⁻¹) using a one-hole spinneret. The diameter (D) of the capillary hole was 0.3 mm, and the ratio of the capillary length L to the capillary diameter (L/D) amounted to 2.

Multifilament Yarn Preparation Using Extruder Spinning Equipment

Melt spinning experiments were carried out using a single screw extruder spinning equipment as presented schematically in Figure 3. The PP/EOC blend was fed into the extruder having three heating zones. After melting of PP/EOC blend, the melt passed the metering pump pressing the molten material through the designed spinneret with 12 capillary holes ($D = 0.25$ mm,

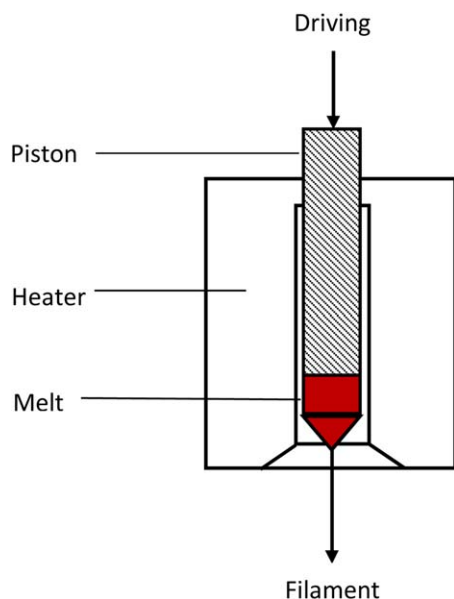


Figure 2. Scheme of piston melt spinning device. [Color figure can be viewed in the online issue, which is available at wileyonlinelibrary.com.]

$L/D = 2$). The total throughput (Q) was adjusted by the rotational speed of the metering pump to 12 g min^{-1} . The filaments cooled down and were wound on bobbins at various take-up velocities (V) in the range from 500 to 3000 m min^{-1} . All fibers were spun without drawing.

Tensile Tests and Mechanical Properties of As-Spun Fibers

The tensile tests were carried out on a tensile testing device (Zwick Roell Z 0.5, Zwick/Roell Company, Germany.) at room temperature (22°C) using fiber lengths of 50 mm , a crosshead speed of 100 mm min^{-1} and an initial force of 0.7 cN . The initial modulus (E_0) was determined between the strain values of 0.05 and 0.25% . The fineness Tt (tex) of the as-spun fibers was first determined by weighing a specific sample length. In addition, the authors calculated its value by the following equation:

$$Tt = \frac{Q}{V} \quad (2)$$

where Q is the total throughput and V is the take-up velocities.

RESULTS AND DISCUSSION

Before evaluating the results of melt spun fiber with different PP/EOC blend ratios, it is worth to note that EIReP induced modifications of molecular architecture of PP/EOC blends at doses of 3 , 6 , and 12 kGy included chain scission of PP, chain branching of EOC, and PP-EOC graft-linking. Due to our latest study,²¹ cross-linking of EOC starts at dose values higher than 18 kGy . Consequently, the authors set the maximum dose during EIReP to 12 kGy in order to avoid any cross-linking of EOC phase in PP/EOC blends leading to problems in their melt spinning.

Melt Spinning Behavior of Toughened PP

The melt spinning process makes great demands on the materials with respect to the molecular mass, dispersity, homogeneity, thermal stability, flow behavior, and ratio between viscous and elastic properties of the melt ($\tan \delta$). The first evaluation of the melt spinnability of PP/EOC blends was done by studying the

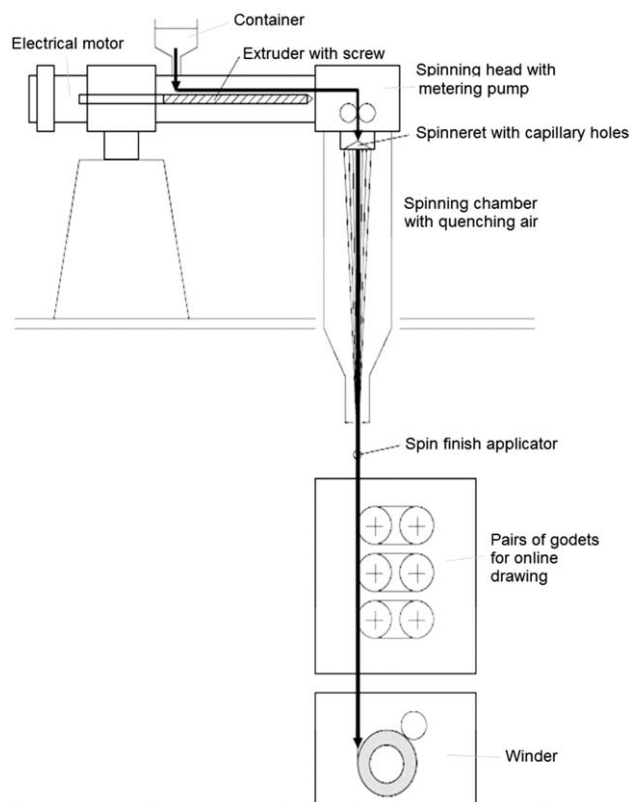


Figure 3. Scheme of melt spinning equipment.

rheological and thermal properties. In a second step, the authors tested the general spinning behavior using a piston single fiber spinning device. Finally, multifilament spinning was tested on an extruder spinning equipment.

Rheological Properties. The investigation of rheological and thermal properties by rheological experiments aims on the evaluation of fiber formation of the PP/EOC blends. The following figures in this section only present the results of unmodified A0 and EIReP-modified A3, A6, and A12 blends with mass the PP/EOC ratios of $97.5/2.5$ because the results of the rheological studies of B and C blends (PP/EOC mass ratios of $95/5$ and $90/10$) show similar features and tendencies. Figure 4 depicts the absolute value of complex viscosity ($|\eta^*|$) and the loss angle

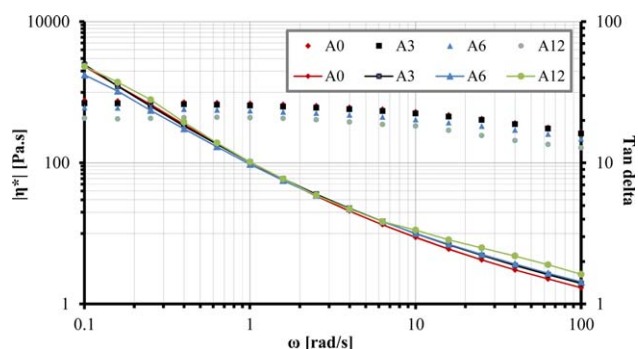


Figure 4. $|\eta^*|$ (only markers) and $\tan \delta$ (straight line with markers) as function of angular frequency (ω) at 200°C . [Color figure can be viewed in the online issue, which is available at wileyonlinelibrary.com.]

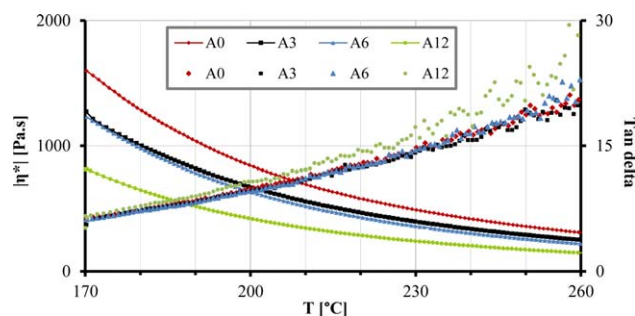


Figure 5. η^* (only markers) and $\tan \delta$ (straight line with markers) as a function of temperature T at 1 rad s^{-1} . [Color figure can be viewed in the online issue, which is available at wileyonlinelibrary.com.]

$\tan(\delta)$ of the A blends as function of the angular frequency ω at 200°C in a log–log plot. All samples show pseudoplastic behavior, that means the viscosity decreases with increasing shear rate. It is clearly seen that the viscosity of the EIREP-modified samples decreases with an increase in absorbed dose. The melt flow behavior of A12 blend (treated at 12 kGy) shows instabilities and degradation effect at low angular frequency, and in general, its viscosity is drastically reduced in comparison to the A0–A6 blends. Figure 5 shows η^* and the loss angle $\tan(\delta)$ of the A blends as function of temperature (T) at a constant angular frequency (ω) of 1 rad s^{-1} . Again, the A12 blend shows remarkable decrease in the complex viscosity and also an unstable molten flow behavior at higher processing temperatures ($>220^\circ\text{C}$). Beyreuther *et al.*¹⁹ suggested that a polymer is well spinnable if the elastic flow properties do not overbalance the viscous ones. This means in other words that the loss angle $\tan(\delta)$ should be not lower than 10 at a frequency of 1 rad s^{-1} in the frequency sweep curve. Therefore, the frequency sweep at different temperatures proves to be as a test of melt spinnability in order to select the optimum temperature and shear rate. At least, there are no general restrictions to anticipate with respect to the melt spinnability of PP/EOC blends obtained from Figures 4 and 5. Figure 6 presents the absolute value of complex viscosity as a function of temperature during the cooling cycle beginning at 240°C , at a cooling rate of 5 K min^{-1} and a fixed angular frequency of 10 rad s^{-1} . The viscosity of untreated standard spinning polymer PP HG455FB is shown in the figures as reference. As expected from the results in Figures 4 and 5,

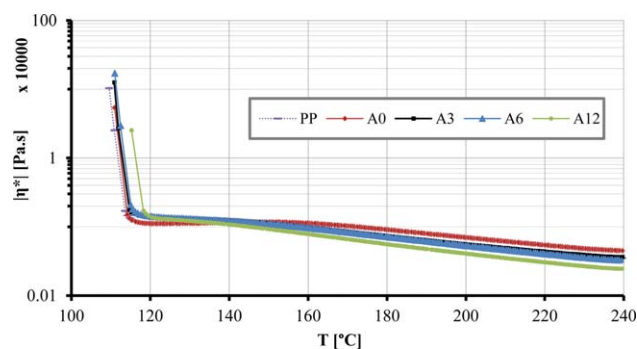


Figure 6. η^* as function of cooling temperature at a cooling rate 5 K min^{-1} and at 10 rad s^{-1} . [Color figure can be viewed in the online issue, which is available at wileyonlinelibrary.com.]

Table I. Absolute Value of Complex Viscosity $|\eta^*|$ of Frequency Sweep Test at an Angular Frequency of 0.1 rad s^{-1} and at a Temperature of 200°C

Blend	$ \eta^* $ (Pa s)	Blend	$ \eta^* $ (Pa s)	Blend	$ \eta^* $ (Pa s)
A0	767	B0	810	C0	890
A3	698	B3	723	C3	786
A6	610	B6	675	C6	722
A12	429	B12	516	C12	625

the viscosity of A0 blend shows a much higher level compared to the reference PP, and the viscosity level of the blends A3, A6, and A12 decreases with an increasing dose under the conditions of decreasing processing temperature starting at 240°C . At least, the A3 and A6 blends show similar viscosity level than the reference PP. The solidification by crystallization starts at temperatures lower than 120°C , and this agrees well to the results of DSC analysis. Furthermore, all blends show good thermal stability during the time sweep measurements.

Finally, Table I presents the results for the absolute value of complex viscosity of PP/EOC blends for the frequency sweep tests at an angular frequency of 0.1 rad s^{-1} and at a temperature of 200°C . As expected, the viscosity of the PP/EOC blends increases with an increased EOC fraction, whereas the viscosity decreases with an increased dose during EIREP due to chain scission of PP. These effects of different PP/EOC blend ratios and doses have to be taken into account for the selecting of adjusted melt spinning temperature.

Thermal Analysis (DSC). The DSC experiments were carried out to study the melting behavior of the modified blends as well as to explore the structural changes that can affect the fiber formation process. The resulting values of melting temperature and crystallinity of PP in the blends are listed in Table II. In the case of EOC phase, no obvious change of the thermal properties of EOC phase was observed. Therefore, the measured dates were not presented. Its average melting, crystallization temperature, and the crystallinity amount to 58°C , 44°C , and 2.3%, respectively. Figure 7 depicts the melting behavior of the PP/EOC blends obtained from DSC scans in second heating. The thermal behavior of PP in the modified blends is comparable to that of unmodified PP. In the case of A and B blends, the crystallinity (X) increases slightly with increased dose. In addition, the melting temperature (T_m) increases slightly for A blends modified with a dose of 3 and 6 kGy. At a dose of 12 kGy, the melting

Table II. Melting Temperature (T_m) and Crystallinity (X) of PP Matrix Phase

Blend	T_m ($^\circ\text{C}$)	X (%)	Blend	T_m ($^\circ\text{C}$)	X (%)	Blend	T_m ($^\circ\text{C}$)	X (%)
A0	161	41	B0	160	44	C0	160	50
A3	164	43	B3	161	46	C3	161	49
A6	165	45	B6	161	47	C6	161	48
A12	159	48	B12	162	47	C12	162	48

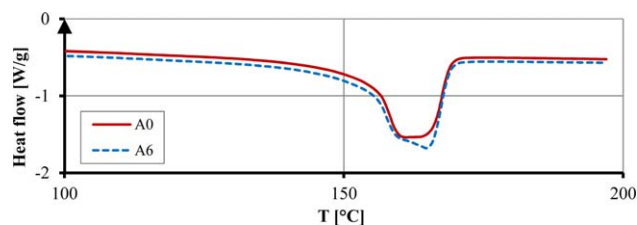


Figure 7. Heat flow versus temperature T at heating rate of 10 K min^{-1} for A0 and A6 blends (second heating scan, exotherm is in direction of arrow). [Color figure can be viewed in the online issue, which is available at wileyonlinelibrary.com.]

temperature is less compared to the unmodified (A) blends. It is worth mentioning that the irradiated blends exhibited slightly broader melting endotherm peaks than the unmodified ones (Figure 7), which may be caused by the existence of altered molecular chain structures. In addition, multiple melting peaks or peak and shoulder were observed for the irradiated samples as (A6) in Figure 7. The cause of this behavior was the melting and the reorganization during heating. The difficulty was the high recrystallization rate of the PP phase. That means high heating rates were necessary to prevent reorganization during heating.

Piston Single Fiber Spinning

The objective of the investigation was to characterize the melt spinning behavior at different temperatures, to estimate the maximum possible take-up velocities, and to determine the resulting pressure of the melt for the capillary hole of the spinneret. Figure 8 presents as an example of the melt pressure P as a function of processing temperature (T) at a throughput of 0.6 g min^{-1} . As expected, the pressure shifted to lower values with increasing processing temperature. In addition, the resulting pressures of all EIReP-modified blends were significantly lower in comparison to the pressure of non-EIReP-modified blends. This is in agreement with the results of rheological investigations. At temperatures higher than 210°C , the pressure reached a critical low value, resulting in more or less melt flow instability (especially at low throughputs). Moreover, the melt pressure showed a strong relationship with the relaxation behavior of the polymer chains. Since the relaxation time of EIReP-modified PP is smaller than the non-EIReP-modified one to a large extent, the polymer in molten phase has more ability to adjust or move permanently to a new position. This advantage of the EIReP-modified blends provided an enhanced stability for the spinning process with more energy saving, that is, higher spinnability at lower processing temperatures. In the case of EIReP-modified A and B blends, all the single fibers could be produced without instabilities, such as melt fracture, high extrudate swell, and filament breakage even at extreme conditions of take-up speed (2000 m min^{-1}) and throughput (0.1 g min^{-1}). The as-spun fibers of A and B blends looked optically smooth and were well spinnable. In contrast, the viscosity gap between PP and EOC phases for EIReP-modified C blends caused flow instabilities, especially at low throughput. These distortions could be optically observed on the filament surfaces during the melt spinning process. At least, all spinning trials were successfully spun at a throughput of 0.6 g min^{-1} up to a take-up velocity of 2000 m min^{-1} .

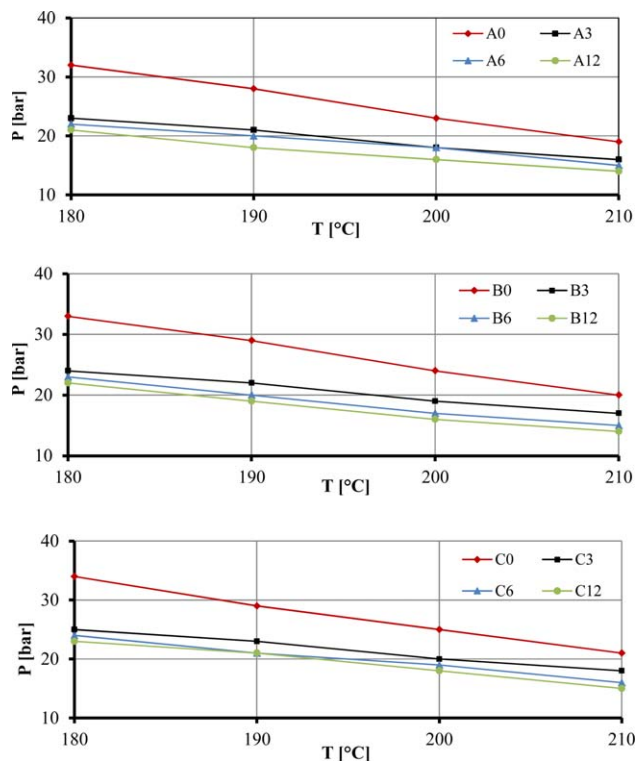


Figure 8. Resulting pressure P during single fiber spinning as a function of spinning temperature T at a throughput of 0.6 g min^{-1} (symbols: measured values). [Color figure can be viewed in the online issue, which is available at wileyonlinelibrary.com.]

Multifilament Spinning

Based on the findings of the single fiber piston spinning trials, the authors determined a stable multifilament spinning process of PP/EOC blends using an extruder spinning equipment. In comparison to previous pure PP trials, special adjustments were made with respect to the temperature guidance of the extruder heating zones and the spinning head. Finally, the authors used following optimized temperatures (Table III).

These adapted temperatures allowed to run a stable multifilament spinning process within the limits of the available melt spinning conditions. The authors continuously increased the take-up velocity with the incremental steps of 100 m min^{-1} at fixed throughput in order to determine the limits of spinnability under the selected conditions of extruder spinning experiments. Table IV summarizes the data of several runs with respect to the maximum achievable take-up velocity (V_{max}), the corresponding maximum draw down ratio (DDR_{max}), and the minimum achievable fineness (T_{tmin}). The condition for the

Table III. Temperature Conditions for Unmodified and EIReP-Modified PP/EOC Blends

Zone	Temperature ($^\circ\text{C}$)
Extruder hot zones	180–190–195
Spinning head	200
Polymer melt	201–202

Table IV. Melt Pressure (P), Maximum Take-Up Velocity (V), and Draw down Ratio (DDR) as well as Minimum Fineness ($T_{t_{\min}}$) for Multifilament Spinning of PP/EOC Blends at a Throughput of 12 g min^{-1}

Blend	P (bar)	V_{\max} (m min^{-1})	DDR_{\max}	$T_{t_{\min}}$ (dtex) of 12 g min^{-1}
A0	59	2600	114	46
A3	55	2800	123	43
A6	48	2300	101	52
A12	39	2600	114	46
B0	59	2600	114	46
B3	51	2600	114	46
B6	50	2900	127	41
B12	49	2700	119	44
C0	58	2600	114	46
C3	54	2600	114	46
C6	53	2700	127	44
C12	49	3000	132	40

maximum take-up velocity (V_{\max}) was a running time of five minutes without fiber breakages.

The maximum draw down ratio is given by

$$\text{DDR}_{\max} = \frac{V_{\max}}{V_0} \quad (3)$$

where (V_0) is the extrusion velocity, depending on the capillary diameter of the spinneret hole and the throughput per hole.

The minimum fineness ($T_{t_{\min}}$) is given by

$$T_{t_{\min}} = \frac{Q}{V_{\max}} \quad (4)$$

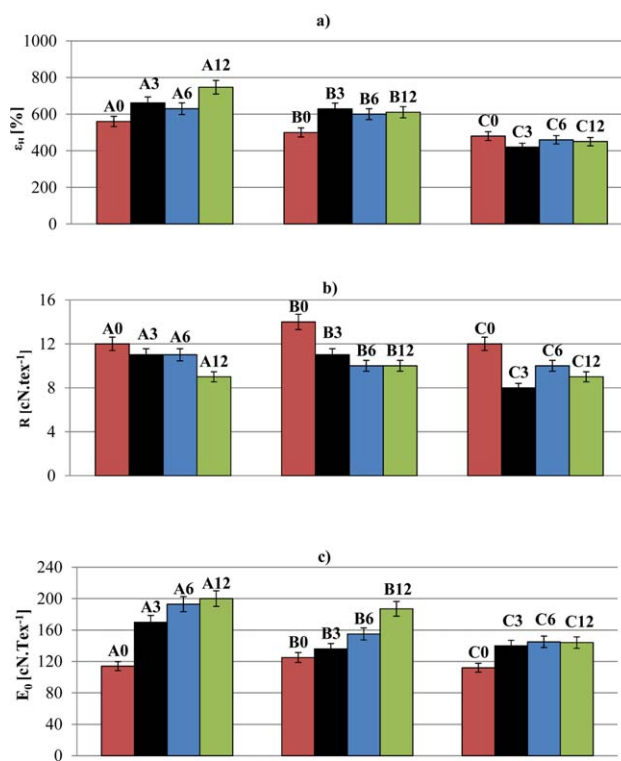
where Q is the total throughput and V_{\max} is the maximum take-up velocity. Based on these results (Table IV), the authors concluded that all PP/EOC blends can be successfully used for the melt spinning of multifilament yarns by means of extruder spinning: The reached maximum possible draw down ratios under optimized conditions were >100 , the minimum achievable finenesses per filament were ≤ 4 dtex. The melt pressure showed the same tendency as in the single fiber spinning experiments.

Textile Properties of As-Spun Multifilament Yarn from PP/EOC Blends

For all test samples, the deviations of the gravimetric measured fineness of the multifilament yarns from the calculated ones can be neglected. At least, the tensile strength measurements were achieved using the calculated fineness in accordance to eq. (2).

Table V. Textile Physical Properties (E_0 , R , and ϵ_H) of Multifilament Yarn at a Take-Up Speed of 500 m min^{-1}

Blend	E_0 (cN tex^{-1})	R (cN tex^{-1})	ϵ_H (%)	Blend	E_0 (cN tex^{-1})	R (cN tex^{-1})	ϵ_H (%)	Blend	E_0 (cN tex^{-1})	R (cN tex^{-1})	ϵ_H (%)
A0	114	12	560	B0	115	13	500	C0	112	12	480
A3	170	11	660	B3	136	11	629	C3	140	10	420
A6	200	11	360	B6	155	10	600	C6	145	9	460
A12	210	10	740	B12	187	9	610	C12	144	8	450

**Figure 9.** Textile physical properties of multifilament at take-up speed of 500 m min^{-1} . (b) Elongation at break (ϵ_H), (b) tenacity (R), and (c) initial modulus (E_0). [Color figure can be viewed in the online issue, which is available at wileyonlinelibrary.com.]

The obtained textile properties of as-spun fibers of PP/EOC blends showed the same typical behavior with respect to an increased take-up velocity as the pure and non-EIReP-modified PP fibers. The higher the take-up velocity is the higher the orientation of the polymer chains. High orientation leads to high initial modulus, high tenacity, and low elongation at break. Nevertheless, the high orientation of polymer chains after melt spinning is lost during the consolidation process. Consequently, the properties of low oriented fibers are of interest for the advanced manufacturing of fiber reinforced thermoplastic composites based on the use of hybrid yarn. Table V and Figure 9 present the textile physical properties of melt spun fibers from PP/EOC blends at low orientation level (take-up velocity: 500 m min^{-1}).

CONCLUSIONS

This work aimed on the preparation of PP/EOC blends with different blend ratios for the subsequent melt spinning process.

Later, the effect of PP/EOC blend ratio and absorbed dose during EIReP on the melt spinning behavior, and performance of PP/EOC blend fibers has been studied. In the design phase of melt-spinnable PP, the authors took into account the demands of melt spinning process on the molecular mass, dispersity, and homogeneity of PP/EOC blends. Consequently, the experimental results of rheological and thermal investigations as well as of spinning tests confirmed the melt-spinnability of EOC toughened PP. In addition, the authors found a significant influence on the amount of EOC and dose absorbed during EIReP on the physical properties of the multifilament. Optimum melt spinning behavior and physical properties of multifilaments were achieved at a PP/EOC blend ratio of 97.5/2.5 and at a dose of 6 kGy. Interestingly, the authors achieved an increase in the initial modulus of about 70% for low oriented PP/EOC fibers which might be of interest for the preparation of fiber reinforced PP. Systematic investigations are in progress in order to understand the reason as well as the mechanism behind this experimental result.

ACKNOWLEDGMENTS

The authors would like to thank Mr. Zschech for the preparation of EOC/PP blends by EIReP and Mr. Smolka and Mr. Häschel for the technical support by the fiber formation process.

REFERENCES

1. Babu, R. R.; Gohs, U.; Naskar, K.; Mondal, M.; Wagenknecht, U.; Heinrich, G. *Macromol. Mater. Eng.* **2012**, *297*, 659.
2. Legge, N. R.; Holden, G.; Schroeder, H. E. *Thermoplastic Elastomers: A Comprehensive Review*; Munich: Hanser Publishers, **1987**.
3. Walton, K. L. *Rubber Chem. Technol.* **2004**, *77*, 552.
4. Drobny, J. G. *Radiation Technology for Polymers*, 2nd ed.; Boca Raton, Florida: USA: CRC Press, **2003**.
5. Naskar, K.; Gohs, U.; Wagenknecht, U.; Heinrich, G. *eXPRESS Polym. Lett.* **2009**, *3*, 677.
6. Rooj, S.; Thakur, V.; Gohs, U.; Wagenknecht, U.; Bhowmick, A. K.; Heinrich, G. *Polym. Adv. Technol.* **2010**, *22*, 2257.
7. Krause, B.; Voigt, D.; Lederer, A.; Auhl, D. *J. Appl. Polym. Sci.* **2006**, *100*, 2770.
8. Krause, B.; Voigt, D.; Lederer, A.; Auhl, D.; Münstedt, H. *Chromatogr. A* **2004**, *1056*, 217.
9. Gohs, U.; Heinrich, G.; Stephan, M.; Volke, S.; Wagenknecht, U. In *Proceedings of the Polymer Processing Society 24th Annual Meeting PPS-24; Italy*, **2008**.
10. Zaharah, A. K.; Yoshii, F.; Makuuchi, K.; Ishikaki, I. *Polymer* **1989**, *30*, 1425.
11. DeNicola, A. J. Jr. Eur. Pat. 0,351,866 (**1989**).
12. Scheve, B. J.; Mayfield, J. W.; DeNicola, A. J. Jr. Eur. Pat. 0,190,889 (**1986**).
13. Scheve, B. J.; Mayfield, J. W.; DeNicola, A. J. U.S. Pat. 4,916,198 (**1990**).
14. Mäder, E.; Rothe, C.; Brünig, H.; Leopold, T. *Engineering Materials* **2007**, *334*, 229.
15. Mäder, E.; Rothe, C. *Chem. Fibers Int.* **2006**, *5*, 298.
16. Babu, R. R.; Naskar, K.; Thakur, V.; Gohs, U.; Wagenknecht, U.; Heinrich, G. *Rad. Phys. Chem.* **2011**, *80*, 1398.
17. Krause, B.; Voigt, D.; Häussler, L.; Auhl, D.; Münstedt, H. *J. Appl. Polym. Sci.* **2006**, *2770*, 100.
18. Noma, T.; Murata, T.; Masubuchi, Y.; Takimoto, J.; Koyama, K. *Polym. Prep. Jpn.* **1997**, *46*, 3829.
19. Beyreuther, R.; Brünig, H.; Vogel, R. *Polymeric Material Encyclopedia: Synthesis, Properties, and Applications*, Vol. 6, 4061; Boca Raton, Florida, USA: CRC Press, **1996**.
20. Zschech, C.; Miersch, F.; Gohs, U.; Heinrich, G. *J. Plast. Technol.* **2016**, *12*, 2.
21. Gohs, U.; Girduškaite, L.; Peitzsch, L.; Rothe, S.; Zschech, C.; Heinrich, G.; Rödel, H. *Adv. Eng. Mater.* **2016**, *18*, 409.